A Reduced Complexity Decoding Scheme for Trellis Coded Modulation

Pisit Charnkeitkong[1] and Thawan Laopetcharat[2]
[1] Faculty of Information Technology,
Rangsit University ,Muang-Ake
Pahonyotin Road, Patumtani 12000, Thailand
e-mail : pisitc@rangsit.rsu.ac.th
[2] Department of Electrical Engineering,
Rangsit University ,Muang-Ake
Pahonyotin Road, Patumtani 12000, Thailand
e-mail : zx432353@rangsit.rsu.ac.th

Abstract: In this paper, we propose a technique used to simplify the trellis diagram, thus, reduce the complexity of Viterbi decoder in term of the number of Compare-Select (CS) operations needs in decoding process. It is shown that if the branch metrics are properly decomposed into orthogonal components. The trellis diagram can be modified that each original state with large number branches terminating to it can be broken into a number of sub-states having smaller number of branches terminating to them. Simulation results shown that the newly proposed technique can be used reduced the complexity of 8 and 16 PSK-TCMs without degrading the BER performance.

1. Introduction

TCM technique is an integration of convolutional coding and multidimensional signal constellations modulation that use to provide reliable, high-data-rate communication over bandwidth-limited channels. Another benefit of TCM is that it can be maximum likelihood decoded with Viterbi algorithm. However, the number of the Compare-Select (CS) operations required in the original Viterbi decoding algorithm increases exponentially with the number of encoder inputs. For the binary channel coding, theis problem is avoided thruough the use of punctured convolutional code, but there is no efficient solution for multi-level signal constellation TCM.

In this paper, we propose a technique used to simplify the trellis diagram, thus reduce the complexity of Viterbi decoder in term of the number of CS operations needs in decoding process. The idea of the newly propose technique is that if branch metrics are properly decomposed into orthogonal components, the trellis diagram can be modified that each original state with large number branches terminating to it can be broken into a number of sub-states having smaller number of branches terminating to them. As a result, the newly obtained trellis diagram is required smaller number ACS operations than that of the original.

The paper is organized as follows. In section 2, the background of TCM is given. In section 3, we propose the idea of how to simplify the trellis diagram of TCM. As an example, based on the proposed technique, the trellis diagram of optimum 4 states, rate 2/3 Ungerboeck 8 PSK-TCM is modified so that the number of Comparison-Select operations required decode 1 information bit is reduced from 6 to 4. In section 5, simulations are performed to evaluate the BER performance of the proposed decoding techniques for the optimum Ungerboeck 8 and 16 PSK-TCM schemes. It is shown that the performance in term of BER of the newly proposed technique is almost the same as that of the ordinary one.

2. Background of TCM

Ungerboeck [1] ha shown that for bandlimited channels substantial coding gains could be achieved by convolutional coding of signal levels (rather than coding of binary source levels). The block diagram of a TCM communication system is depicted in Figure 1. Constellation mapper maps the codeword to signal in order to increase the Euclidean distance of code sequence based on a heuristic technique called set portioning [1].

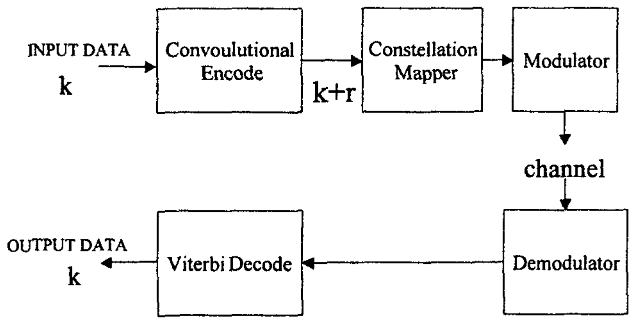

Figure1: Trellis Coded Modulation

Viterbi Algorithm is a Maximum Likelihood Decoding (MLD) technique that estimates the path that the encoded signal traversed through the trellis by associating with each branch of the trellis a branch metric and finding the path whose total metric is minimized. After processing through the matched filter and sampling at $t=JT$, $J=0,1,2,\ldots$ the n-th state s_J^n stores the survivor path and its metric [4]

$$D_J^2(s_J^n) = \min_{\forall x}\left\{\left[r_J - \tilde{y}_J(s_J^n, s_{J-1}^x)\right]^2 + D_{J-1}^2(s_{J-1}^x)\right\} \quad (1)$$

where $\tilde{y}_J(s_J^n, s_{J-1}^x)$ is the estimate transmitted branch signal from x-th state s_{J-1}^x at time J-1 to the n-th state s_J^n at time J, and r_J is the received signal at time J.

For a 2^m states, rate k/n TCM, the number of branches leaving and entering each state is 2^k and, thus, the number of CS operations needed is

$$\frac{(2^k-1)}{k}2^m \quad \text{Operations / bit} \qquad (2)$$

It should be noted here that the number of branches leaving/entering each states and the number of CS operations increase exponentially with the number of encoder input *k*. However, the bandwidth efficiency of TCM tends to increase with the number of inputs *k* and the number of states 2^m. For the BPSK, the problem in decoding convolutional code with large input *k* is avoided through using of the punctured convolutional code, but there is no efficient solution for multi-level signal constellation TCM.

As an example, Figure 2 shows the encoder and the trellis diagram of the optimum 4 states, rate 2/3 Ungerboeck 8 PSK-TCM.

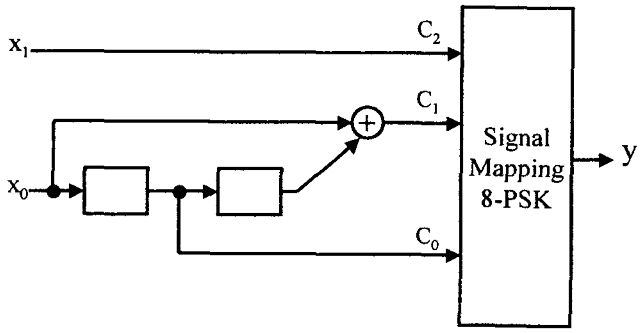

(a) TCM Encoder

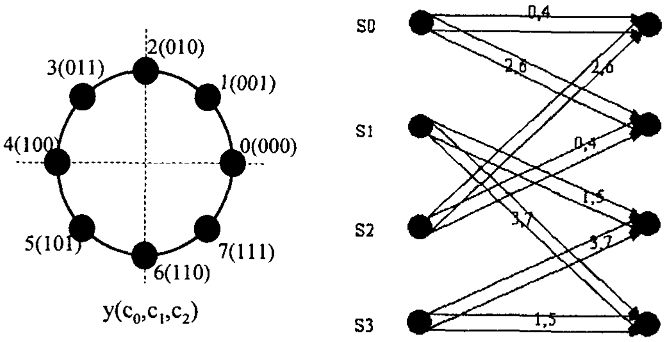

(b) Trellis Diagram and Signal Constellation

Figure 2: The 4-state, rate 2/3 Ungerboeck 8 PSK-TCM

The survivor metrics M_i^J for states *i*, *i*=0,1,2 and 3 at time *J* are given by

$$M_0^J=\min(M_0^{J-1}+d_0^2, M_0^{J-1}+d_4^2, M_2^{J-1}+d_2^2, M_2^{J-1}+d_6^2) \quad (3.a)$$

$$M_1^J=\min(M_0^{J-1}+d_2^2, M_0^{J-1}+d_6^2, M_2^{J-1}+d_0^2, M_2^{J-1}+d_4^2) \quad (3.b)$$

$$M_2^J=\min(M_1^{J-1}+d_1^2, M_1^{J-1}+d_5^2, M_3^{J-1}+d_3^2, M_3^{J-1}+d_7^2) \quad (3.c)$$

$$M_3^J=\min(M_1^{J-1}+d_3^2, M_1^{J-1}+d_7^2, M_3^{J-1}+d_1^2, M_3^{J-1}+d_5^2) \quad (3.d)$$

where d_j^2 is the branch metric corresponding to signal *j*, *j*=0,1,2, ... , 7

$$d_j^2=[r_I-m_I(j)]^2+[r_Q-m_Q(j)]^2 \quad (4)$$

here, r_I and r_Q are in-phase and quadrature componentsof the received signal *r*, and $m_I(j)$ and $m_Q(j)$ are in-phase and quadrature components of estimate branch signal *j*.

From Figure 2 and (3), the number of branches leaving (entering) each state and the number of CS operations needed to decode an information bit are 4 and 6, respectively.

3. A Reduced Complexity Decoding Technique

In this section, we propose a technique used to simplify the trellis diagram, thus reduce the complexity of Viterbi decoder in term of the number of CS operation needed in decoding process.

The idea of the newly propose technique is that if the received signal and the branch signals are properly decomposed into orthogonal components. The branch metrics can also be decomposed into orthogonal components too. This allows us to modify the survivor metric calculation statement, such as reducing the number of different branch metrics, regrouping the terms into simpler sub-statements of CS operation. Surprisingly, the newly obtained trellis diagram have more decoding stages, but requires smaller number of branch entering to them, thus requires smaller number of total CS operations in decoding process.

3.1 Simplifying the 4 states, rate 2/3 Ungerboeck 8 PSK-TCM

As an example, let consider 8 PSK-TCM shown in Figure 2. From Figure 2 and (3), it should be noted that there are 2 different groups of 4 signals terminating to each state. The 2 groups of signals are A= {0,4,2,6} and B={1,5,3,7}, where signal group A entering S0 and S1 while signal group B entering S2 and S3.

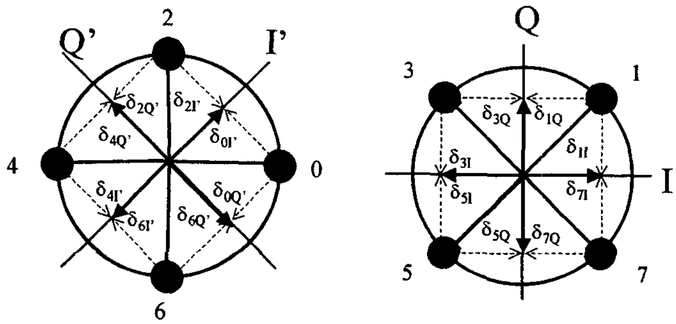

Figure 3. Two groups of 8-PSK signals

Consider signal group B, let δ_{jI} and δ_{jQ} be the components of signal *j*, *j*= 1,3,5,7 that corresponding to axes I and Q, respectively. Hence, the branch metric (4) corresponding to signal *j*, *j*=1,3,5, 7 can be rewritten as

$$d_j^2=[r_I-\delta_{jI}]^2+[r_Q-\delta_{jQ}]^2$$
$$d_j^2=d_{jI}^2+d_{jQ}^2 \qquad (5)$$

where d_{iI}^2 and d_{iQ}^2 are squared Euclidean distances corresponding to axes I and Q, respectively. Similarly, for signal group A, let $\delta_{jI'}$ and $\delta_{jQ'}$ be the components of signal j, j= 0,2,4,6 that corresponding to axes I' and Q', respectively. The branch metric (4) corresponding to signal j, j=1,3,5, 7 can be rewritten as

$$d_j^2 = [r_{I'} - \delta_{jI'}]^2 + [r_{Q'} - \delta_{jQ'}]^2$$
$$d_j^2 = d_{jI'}^2 + d_{jQ'}^2 \qquad (6)$$

where $d_{iI'}^2$ and $d_{iQ'}^2$ are squared Euclidean distances corresponding to axes I' and Q', respectively. Substituting (5) and (6) into (3), we have

$$M_0^J = \min(M_0^{J-1}+(d_{0I'}^2+d_{0Q'}^2), M_0^{J-1}+(d_{4I'}^2+d_{4Q'}^2), M_2^{J-1}+(d_{2I'}^2+d_{2Q'}^2), M_2^{J-1}+(d_{6I'}^2+d_{6Q'}^2)), \quad (7.a),$$
$$M_1^J = \min(M_0^{J-1}+(d_{2I'}^2+d_{2Q'}^2), M_0^{J-1}+(d_{6I'}^2+d_{6Q'}^2), M_2^{J-1}+(d_{0I'}^2+d_{0Q'}^2), M_2^{J-1}+(d_{4I'}^2+d_{4Q'}^2)), \quad (7.b),$$
$$M_2^J = \min(M_1^{J-1}+(d_{1I}^2+d_{1Q}^2), M_1^{J-1}+(d_{5I}^2+d_{5Q}^2), M_3^{J-1}+(d_{3I}^2+d_{3Q}^2), M_3^{J-1}+(d_{7I}^2+d_{7Q}^2)), \quad (7.c),$$
$$M_3^J = \min(M_1^{J-1}+(d_{3I}^2+d_{3Q}^2), M_1^{J-1}+(d_{7I}^2+d_{7Q}^2), M_3^{J-1}+(d_{1I}^2+d_{1Q}^2), M_3^{J-1}+(d_{5I}^2+d_{5Q}^2)). \quad (7.d).$$

From Figure 3, it is clear that for signal group B

$$\delta_{1I} = \delta_{7I},\ \delta_{1Q} = \delta_{3Q}$$
$$\delta_{3I} = \delta_{5I},\ \delta_{5Q} = \delta_{7Q}, \qquad (8)$$

and for signal group A

$$\delta_{0I'} = \delta_{2I'},\ \delta_{0Q'} = \delta_{6Q'}$$
$$\delta_{4I'} = \delta_{6I'},\ \delta_{2Q'} = \delta_{4Q'}. \qquad (9)$$

From (5), (6), (8) and (9) we obtain the following relations

$$d_{1I}^2 = d_{7I}^2,\ d_{1Q}^2 = d_{3Q}^2$$
$$d_{3I}^2 = d_{5I}^2,\ d_{5Q}^2 = d_{7Q}^2$$
$$d_{0I'}^2 = d_{2I'}^2,\ d_{2Q'}^2 = d_{4Q'}^2$$
$$d_{4I'}^2 = d_{6I'}^2,\ d_{0Q'}^2 = d_{6Q'}^2 \qquad (10)$$

Substituting (10) into (7), we have

$$M_0^J = \min(M_0^{J-1}+(d_{0I'}^2+d_{0Q'}^2), M_0^{J-1}+(d_{4I'}^2+d_{2Q'}^2), M_2^{J-1}+(d_{0I'}^2+d_{2Q'}^2), M_2^{J-1}+(d_{4I'}^2+d_{0Q'}^2)), \quad (11.a).$$
$$M_1^J = \min(M_0^{J-1}+(d_{0I'}^2+d_{2Q'}^2), M_0^{J-1}+(d_{4I'}^2+d_{0Q'}^2), M_2^{J-1}+(d_{0I'}^2+d_{0Q'}^2), M_2^{J-1}+(d_{4I'}^2+d_{2Q'}^2)), \quad (11.b).$$
$$M_2^J = \min(M_1^{J-1}+(d_{1I}^2+d_{1Q}^2), M_1^{J-1}+(d_{3I}^2+d_{5Q}^2), M_3^{J-1}+(d_{3I}^2+d_{1Q}^2), M_3^{J-1}+(d_{1I}^2+d_{5Q}^2)), \quad (11.c).$$
$$M_3^J = \min(M_1^{J-1}+(d_{3I}^2+d_{1Q}^2), M_1^{J-1}+(d_{1I}^2+d_{5Q}^2), M_3^{J-1}+(d_{1I}^2+d_{1Q}^2), M_3^{J-1}+(d_{3I}^2+d_{5Q}^2)). \quad (11.d).$$

Consider (11.a), the 1st and the 4th terms have common branch metric $d_{0I'}^2$, while the 2nd and 3rd terms have common branch metric $d_{4I'}^2$. This allows us to calculate

$$\min(M_0^{J-1}+d_{0Q'}^2, M_2^{J-1}+d_{2Q'}^2) \text{ and}$$
$$\min(M_0^{J-1}+d_{2Q'}^2, M_2^{J-1}+d_{0Q'}^2)$$

first, then adding $d_{0I'}^2$ and $d_{4I'}^2$ to the results, respectively, and finally select the minimum of the two. That is, (11.a) can be rewritten as

$$M_0^J = \min\{\min(M_0^{J-1}+d_{0Q'}^2, M_2^{J-1}+d_{2Q'}^2)+d_{0I'}^2, \min(M_0^{J-1}+d_{2Q'}^2, M_2^{J-1}+d_{0Q'}^2)+d_{4I'}^2\} \quad (12.a)$$

Similarly, for (11.b), (11.c) and (11.d), we have

$$M_1^J = \min\{\min(M_0^{J-1}+d_{2Q'}^2, M_2^{J-1}+d_{0Q'}^2)+d_{0I'}^2, \min(M_0^{J-1}+d_{0Q'}^2, M_2^{J-1}+d_{2Q'}^2)+d_{4I'}^2\} \quad (12.b)$$
$$M_2^J = \min\{\min(M_1^{J-1}+d_{1Q}^2, M_3^{J-1}+d_{5Q}^2)+d_{1I}^2, \min(M_1^{J-1}+d_{5Q}^2, M_3^{J-1}+d_{1Q}^2)+d_{3I}^2\} \quad (12.c)$$
$$M_3^J = \min\{\min(M_1^{J-1}+d_{1Q}^2, M_3^{J-1}+d_{5Q}^2)+d_{3I}^2, \min(M_1^{J-1}+d_{5Q}^2, M_3^{J-1}+d_{1Q}^2)+d_{1I}^2\} \quad (12.d)$$

The operation corresponding to (12) can be described by the trellis diagram shown in Figure 4.

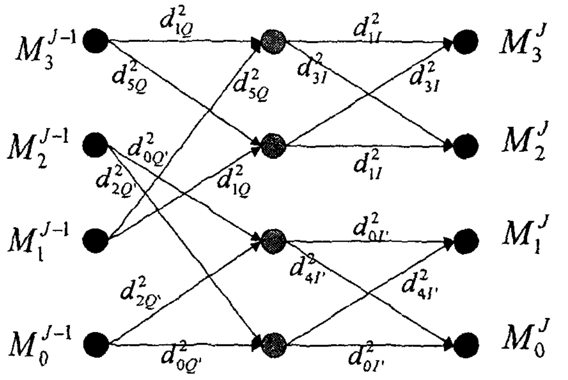

Figure 4. Modified 4-state 8 PSK-TCM trellis diagram

In Figure 4, the trellis diagram has only 2 branches leaving and entering each state. Thus, the number of CS operations required is reduced to 4 per information bit. In a similar way, the trellis diagram of the optimum 8 states rate 3/4

Ungerboeck 16 PSK-TCM [1] can be simplified as shown in Figure 5. As a result, the number of CS operations need to decode this 16 PSK-TCM is reduced from 18.67 to 8 per information bits.

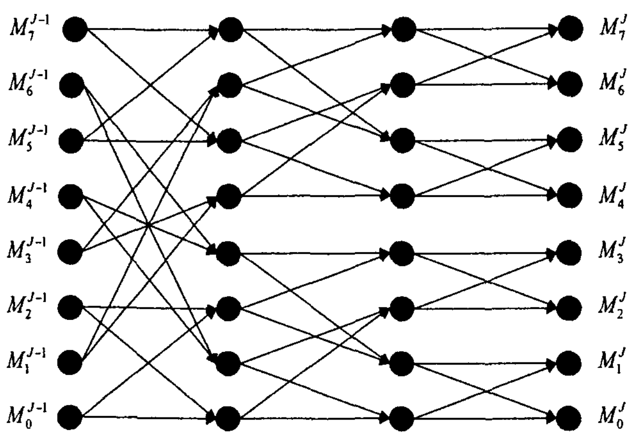

Figure 5. Modified 8-state 16 PSK-TCM trellis diagram

4. Simulation Results

Computer simulations, shown in Figure 6, are performed to evaluate BER performance in term of the required SNR for AWGN channel of the newly proposed technique. It is clear from the results that the newly proposed technique achieves almost the same coding gain as the original Viterbi decoding scheme with smaller number CS operations.

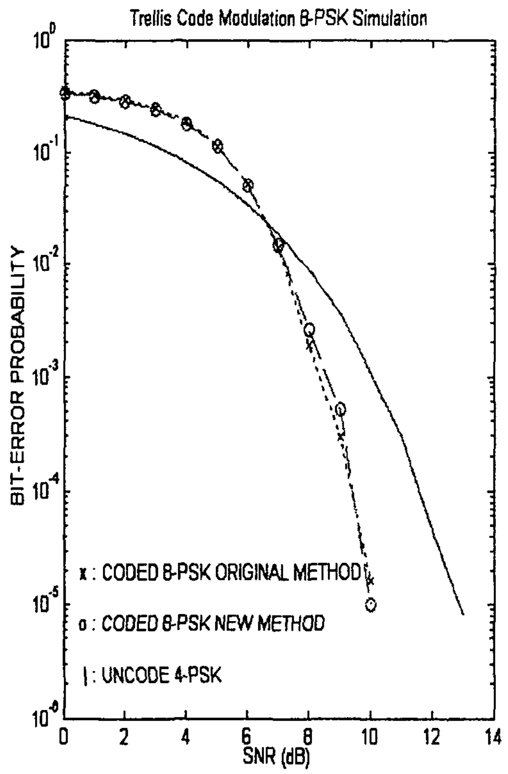

Figure 6. BER performance of 4 states, rate 2/3 Ungerboek 8-PSK-TCM

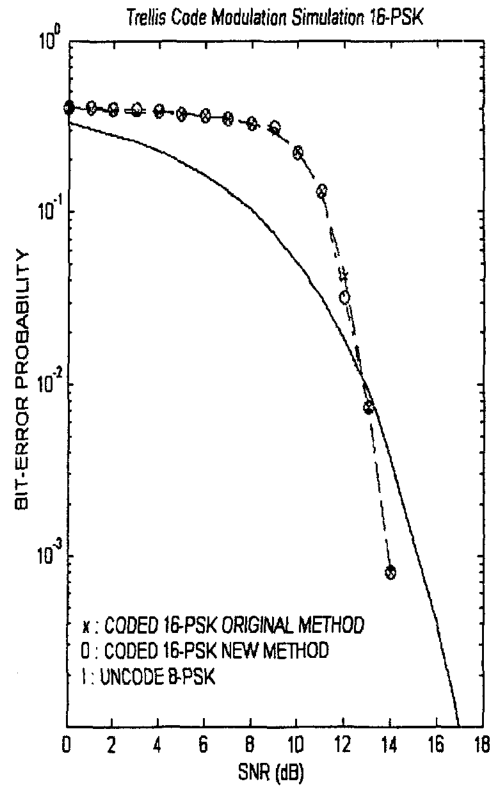

Figure 7. BER performance of 8 states, rate 3/4 Ungerboek 16-PSK-TCM

5. Conclusion

In this paper, a technique used to simplified the trellis diagram, thus reduce the complexity of Viterbi decoder in term of the required number of CS operations is proposed. The proposed technique properly decomposes the branch metrics are into orthogonal components. This allow us to modify trellis diagram that each original state with large number branches terminating to it can be broken into a number of sub-states having smaller number of branches terminating to them. Consequently, the total numbers of required CS operations are significantly reduced. Simulation results shows that, for optimum 8 and 16 PSK-TCMs, the newly proposed technique give the same BER performance as that of the original Viterbi decoding technique.

References

[1] G. Ungerboeck, “Channel Coding with Multilevel/Phase Signals," IEEE Trans. Info. Theory, vol. IT-28,1982, pp. 55-67.

[2] G. Ungerboeck, ‘‘Trellis–coded modulation with redundant signal sets part I: troduction,’’ IEEE Commun. Mag., vol. 25, pp. 5–11, Feb. 1987.

[3] G. Ungerboeck, ‘‘Trellis–coded modulation with redundant signal sets part II: State of the Art,’’ IEEE Commun. Mag., vol. 25, pp. 5–11, Feb. 1987.

[4] Stephen B. Wicker , Error Control Systems for Digital Communication and Storage Prentice Hall Englewood cliffs, NJ 07632.